RESEARCH ARTICLE

Soft rot pathogen *Dickeya dadantii* 3937 produces tailocins resembling the tails of *Enterobacteria* bacteriophage P2

Short title: Tailocins of *Dickeya dadantii* 3937

Marcin Borowicz[a], Dorota M. Krzyżanowska[a], Magdalena Narajczyk[b], Marta Sobolewska[a], Magdalena Rajewska[c], Paulina Czaplewska[d], Katarzyna Węgrzyn[e] and Robert Czajkowski[a,*]

[a] Laboratory of Biologically Active Compounds, Intercollegiate Faculty of Biotechnology of UG and MUG, University of Gdansk, A. Abrahama 58, 80-307 Gdańsk, Poland;

[b] Laboratory of Electron Microscopy, Faculty of Biology, University of Gdansk, Wita Stwosza 59, 80-308 Gdansk, Poland;

[c] Laboratory of Plant Microbiology, Intercollegiate Faculty of Biotechnology of UG and MUG, University of Gdansk, Antoniego Abrahama 58, 80-307 Gdansk, Poland;

[d] Laboratory of Mass Spectrometry-Core Facility Laboratories, Intercollegiate Faculty of Biotechnology of UG and MUG, University of Gdansk, Antoniego Abrahama 58, 80-307 Gdansk, Poland;

[e] Laboratory of Molecular Biology, Intercollegiate Faculty of Biotechnology of UG and MUG, University of Gdansk, Antoniego Abrahama 58, 80-307 Gdansk, Poland

***** Correspondence: robert.czajkowski@ug.edu.pl; phone: 0048 58 523 6333

Abstract

Phage tail-like particles, known as tailocins, are sophisticated nanomolecular machines with bactericidal activity. They are produced by various bacteria to gain fitness advantages in the environment, and hence they play a critical role in bacterial ecology across all known habitats. Here we characterized phage tail-like particles produced by *Dickeya dadantii* strain 3937 – one of the widest-characterized members of plant pathogenic Soft Rot *Pectobacteriaceae* (SRP). Tailocins were induced from *D. dadantii* strain 3937 cells with mitomycin C and visualized and characterized with microscopic techniques (TEM and AFM). They were ca. 166 nm long, tubes surrounded by contractive sheaths with baseplates with tail fibers at one end. Furthermore, we identified a 22-kb cluster in the genome of *D. dadantii* 3937 involved in their synthesis that expressed high homology to the cluster coding for the tail of the Enterobacteriophage P2. The *D. dadantii* 3937 tailocins were named dickeyocins P2D1 (=phage P2-like dickeyocin 1). P2D1 were prone to inactivation by pH (3.5 – 12), temperature (4 – 50 ºC), and elevated osmolarity (NaCl concentration: 0.01 – 1 M). P2D1 could kill different *Dickeya* spp.; however, they were unable to kill any strain of *Pectobacterium* spp. tested. Likewise, they were not toxic to *Caenorhabditis elegans*.

Keywords:

bacteriophage, phage tail, tailocin, *Erwinia chrysanthemi*, bacteriocin, bacteria-bacteria interactions, *Caenorhabditis elegans*

Introduction

Under natural conditions, various bacterial species inhabit shared environments developing spatial and temporal interspecies associations and communities with complex networks of interactions (*1, 2*). In such communities, a particular member needs to continuously compete for limited resources (i.e., scarce nutrients and limited space) with virtually all other members of the community to gain a competitive edge (*3, 4*). Given such challenging living conditions, bacteria evolve diverse strategies to outcompete both closely and distantly related microbes (*5*). Such strategies, although employing a broad range of activities, may overall be divided into two large groups: an indirect, exploitative competition that occurs through the consumption of resources and direct, interference competition, where individual cells directly damage one another, limiting their lifespan (*6*). Whereas exploitative competition depends primarily on the utilization of limited resources by one strain restricting its supplies to the competitor, interference competition relies on producing various antimicrobials that aim to kill the opponent cells (*7*). These antimicrobials include but are not limited to, broad-spectrum antibiotics, toxins, contact-dependent inhibition, effectors transported via type VI secretion system (T6SS effectors), low molecular weight bacteriocins, and phage tail-like particles (*5, 8*). One bacterial cell may often produce and use several such systems to gain fitness advantages in the environment (*7*). Among the systems bacteria exploit to fight competitive microbes, phage tail-like particles are now receiving considerable and increasing attention (*9, 10*).

Phage tail-like particles are syringe-like nanomolecular machines evolutionary and morphologically related to bacteriophage tails, type VI secretion systems, and extracellular contractile injection systems (*10*). These particles, known as high molecular weight bacteriocins or, in short, tailocins, are chromosomally encoded and ribosomally synthesized toxins that usually express a narrow-killing range being able to interact with closely-related bacterial species occupying the same niche (*9*). Their action involves recognizing the sensitive bacterial cell, adsorption to its surface, and puncturing the cell envelope, which

leads to depolymerization of the cell membrane and, ultimately, the death of the attacked cell (*11*).

Tailocins are classified into two distinct families: rigid and contractile (R-type) and noncontractile but flexible particles (F-type) (*12*). The R-type tailocins express similarity to tails of P2 or T-even bacteriophages of the family *Myoviridae* infecting *Escherichia coli*. In contrast, the F-type phage tail-like particles resemble flexible tails of well-known bacteriophage lambda (λ) belonging to the family *Siphoviridae*. Although phage tail-like particles exhibit remarkable morphological similarity to bacteriophage tails of the *Myoviridae* and *Siphoviridae* viruses, it is believed now that they have evolved independently from bacteriophages and should not be considered exclusively domesticated prophages or phage remnants that bacteria harness for their advantage (*10*).

The presence of phage tail-like particles was demonstrated both in Gram-negative and Gram-positive bacterial species, including saprophytic bacteria residing in various environments, human and animal pathogens, as well as plant-associated (beneficial and pathogenic) bacteria (*13-17*). Till present, tailocins have been the best characterized in the case of bacteria belonging to *Pseudomonas* species (*18*). There are, however, reports of phage tail-like particles isolated from *Clostridioides* spp., *Serratia* spp., *Xenorhabdus* spp., *Burkholderia* spp., *Kosakonia* spp., *Budvicia* spp., *Pragia* spp., *Pectobacterium* spp. as well as from other bacteria.

The omnipresence of tailocins in phylogenetically unrelated bacterial genera suggests these particles may be of vital importance for both bacterial competition and fitness in various habitats (*10*). However, the ecological role of phage tail-like particles in the natural environment of the producer has received so far little attention, especially in the case of plant-pathogenic bacteria residing in agricultural fields. This topic is important given the diversity of conditions such bacteria encounter in these settings. Indeed, no broad studies have focused on phage tail-like particles in Soft Rot *Pectobacteriaceae* (SRP) bacteria (*19*), which, due to their lifestyle, have particularly complex spatial and temporal interactions with varied environments (*20-22*).

Plant pathogenic SRP (consisting of *Pectobacterium* spp., *Dickeya* spp., and *Musicola* spp., formerly characterized as pectinolytic *Erwinia* spp.) are a valuable model for studying the role of the phage tail-like particles in the environment. SRP bacteria are widespread in various ecological niches, including rain and surface water, natural and agricultural bulk and rhizosphere soils, sewage, the exterior and interior of host and non-host plants as well as the surface and interior of insects (*19*). Because of the diverse environments in which SRP bacteria may be found, these pathogens may encounter various other bacteria with whom they must efficiently compete for limited resources.

This study aimed to assess the presence and activity of phage tail-like particles induced and isolated from pectinolytic *Dickeya dadantii* strain 3937 (*23*). *D. dadantii* 3937 (formerly *Erwinia chrysanthemi* strain 3937 and *Pectobacterium chrysanthemi* strain 3937 (*24*)) is a well-known necrotrophic plant pathogen that causes soft rot disease symptoms in a variety of crops, ornamental, and other nonfood plants worldwide (*25*). For several decades strain 3937 was widely used as a potent model system for research on the molecular biology and pathogenicity of bacteria belonging to Soft Rot *Pectobacteriaceae (26, 27)*. Strain 3937 remains, until today, the most studied strain of all *Dickeya* species known to date, however, it has never been studied in the context of production of phage tail-like particles and their role.

Here, we characterized in detail previously unknown tailocin produced by *D. dadantii* strain 3937, and we put forward a hypothesis that phage tail-like particles (tailocins) are important for competitive fitness in plant pathogenic *Dickeya* spp., including *D. dadantii*.

Materials and Methods

Bacterial strains and culture conditions

All bacterial strains included in this study are listed in Supplementary Table S1. Bacteria were routinely propagated in liquid Trypticase Soy Broth (TSB, Oxoid) or on solid Trypticase Soy Agar (TSA, Oxoid) at 28 ºC for 24 h. Liquid cultures were agitated during incubation (120 rpm). When required, bacterial cultures were supplemented with kanamycin (Sigma-Aldrich) to a final concentration of 50 µg mL^{-1}.

Induction, purification, and concentration of phage tail-like particles from *Dickeya dadantii* 3937 culture

D. dadantii strain 3937 was grown overnight (ca. 16 h) in TSB at 28 ºC with shaking (120 rpm). The cultures were then rejuvenated by diluting them 1:40 in 250 mL of fresh TSB medium. The diluted culture grew for 2.5 hours under the same conditions. Such prepared 3937 cultures were then supplemented with mitomycin C (Abcam, Poland) to a final concentration of 0.1 µg mL^{-1} to induce the production of phage tail-like particles. Following mitomycin C treatment, the cultures were incubated for another 24 h at 28 ºC with shaking (120 rpm). After this time, bacterial cells were removed by centrifugation (10 min, 8 000 RCF), and the supernatant containing putative phage tail-like particles was collected and filtered through a sterile 0.2 µm PES (polyether sulfone) membrane filter using the Nalgene Rapid-Flow Sterile Disposable Filter Units (Thermo Fisher Scientific). Finally, to precipitate phage tail-like particles, PEG-8000 (Promega) was added to the filtrate to a final concentration of 10%, and the sample was incubated at 4 °C on a magnetic stirrer for the next 16-24 h. The phage tail-like particles were collected by centrifugation (1 h, 16 000 RCF, 4 °C) and resuspended in 5 mL of Phosphate Buffered Saline (PBS, pH 7.2, Sigma-Aldrich). The resulting pellet was resuspended in 1/10 of the initial volume of the initial sample. Between analyses, the purified phage tail-like particles were stored at 4 °C.

Initial qualitative screen of phage tail-like particles for the bactericidal activity

The activity of the purified and concentrated phage-tail-like particles was initially tested qualitatively on a limited panel of bacterial strains (=17 strains), including *D. dadantii* DSM 18020, *D. dadantii* 3937, *D. chrysanthemi* NCPPB 402, *Musicola paradisiaca* NCPPB 2511, *D. dianthicola* NCPPB 3534, *D. dadantii* NCPPB 3537, *D. solani* D s0432-1, *D. zeae* NCPPB 3531, *D. chrysanthemi* NCPPB 3533, *D. dianthicola* IPO 980, *D. oryzae* CSL RW192, *D. solani* MK16, *Dickeya* sp. MK7, *D. solani* GBBC 2040, *D. fangzhongdai* DSM 101947, *P.*

atrosepticum SCRI1043, and *P. parmentieri* SCC3193 (Supplementary Table S1) using a spot test assay as described before (*28, 29*).

Microscopic imaging

Phage tail-like particles were imaged using both transmission electron microscopy (TEM) and atomic force microscopy (AFM), as described earlier (*30*). TEM analyses were done at the Laboratory of Electron Microscopy (Faculty of Biology, University of Gdansk, Poland). For TEM analysis, phage tail-like particles obtained as described above were adsorbed onto carbon-coated grids (GF Microsystems), stained with 1.5% uranyl acetate (Sigma-Aldrich), and directly visualized with an electron microscope (Tecnai Spirit BioTWIN, FEI) using a previously described protocol (*31*). At least ten images were taken for each preparation to estimate the diameters of the phage tail-like particles. For the AFM analysis, purified and PEG-concentrated phage tail-like particles were used directly without further preparations. AFM imaging was conducted in air mode using the Bioscope Resolve microscope (Bruker), in ScanAsyst (Peak Force Tapping) mode, employing the SCANASYST-AIR probes (f0 7.0 kHz, diameter <12 nm, k: 0.4 N/m) as described earlier (*32*). Similarly, as described for TEM analysis, for AFM, at least ten images were taken for each preparation to estimate the diameters of the phage tail-like particles.

Determination of the concentration of phage tail-like particles

To estimate the concentration of tailocins, three independent methods were applied.

Direct particle count with NanoSight NS300

NanoSight NS300 instrument (Malvern Panalytical), equipped with an sCMOS camera and a Blue488 laser, was used to directly assess the concentration and size distribution of phage tail-like particles obtained after induction and purification, as described above. To get within the optimal measuring range, the tailocin samples were diluted 1000 times in sterile PBS

buffer pH 7.2 (Sigma-Aldrich). The camera gain was set to 14, the number of captures per sample equaled 5, each lasting 60 s, and the detection threshold was set to 5 as suggested by the manufacturer. Measurements were conducted at room temperature (ca. 22-23 °C). Three biological replicates were used to determine the concentration and size distribution of the obtained tailocins, and the results were averaged for further analysis.

Semiquantitative estimation by a spot test (28)

Samples interrogated for phage tail-like particles were serially 2-fold diluted in PBS pH 7.2 (Sigma-Aldrich). Two µl of each dilution were spotted onto TSA plates overlayed with 15 ml of soft top agar (Nutrient Broth (NB, Oxoid) with 7 g L^{-1} agar). Before pouring, the soft top agar was cooled to 45 °C and inoculated with 250 µl of an overnight culture of a tailocin indicator strain (susceptible strain *Musicola paradisiaca* NCPPB 2511). Plates were incubated overnight at 28 °C. The highest dilutions of phage tail-like particles still able to cause cell lysis, visible as plaques (halos) in the bacterial lawn in soft top agar, were determined. Each tailocin dilution was tested in triplicates and the entire experiment was repeated two times with the same setup. The reciprocal of the highest dilution causing a visible plaque was defined as the value of the relative activity in arbitrary units (= 1 AU).

Poisson distribution killing method (28)

Phage tail-like particles were also quantified using the Poisson distribution killing method based on the protocol described by (*28*) and initially introduced by (*33, 34*). This method is based on the number of bacteriocidal events, the latter being related to the number of bacterial survivors in a population with a known initial cell count. For that, ten µl of undiluted and 10-times diluted samples tailocins obtained as described earlier were added to 100 µL of an overnight TSB (Oxoid) culture of a susceptible strain *Musicola paradisiaca* NCPPB 2511 (10^8 CFU mL^{-1}) and incubated for 40 min at 28 °C and with shaking (120 rpm). For the negative control, PBS pH 7.2 was used instead of the tailocins suspension. Each combination was tested in triplicates. After the incubation, the suspensions were serially diluted up to 10^{-7} in PBS and plated in triplicates on TSA plates. The colonies that emerged

following overnight incubation at 28 °C were used to calculate the bacterial survival ratio (*S*) in the treated samples compared to the negative control (incubated with PBS). The survival ratio was calculated as the number of viable bacteria in a sample incubated with phage tail-like particles divided by the number of viable bacteria in negative control measured after incubation. The possible average number of lethal events per bacterial cell (*m*) was calculated as $m = -\ln(S)$. Finally, the total number of active killing particles per milliliter (based on the assumption that phage tail-like particles adsorption to bacterial cells in each sample was quantitative within the first 40 min incubation period) was calculated by multiplying *m* by the initial number of bacterial cells per milliliter (CFU mL^{-1}).

Target range of the phage tail-like particles isolated from *D. dadantii* 3937

Fifty-two bacterial strains were surveyed for sensitivity to phage tail-like particles induced from *D. dadantii* strain 3937. These included 41 strains representing different species and subspecies of *Dickeya* and *Pectobacterium*, as well as 7 other bacterial strains belonging to the *Enterobacteriaceae* family, 3 *Pseudomonas* spp., and a single strain of *Staphylococcus aureus* representing Gram-negative bacteria (Table S1). Overnight cultures of the investigated strains were prepared in 1 mL aliquots of TSB in 2 mL microcentrifuge tubes (Eppendorf). The tubes with inoculated medium were incubated horizontally with shaking (120 rpm) at 28 ºC for 16-24 h. The overnight cultures were used as an inoculum in a spot test carried out on 48-well plates (Greiner). Briefly, 10 µL of the inoculum was transferred to each well of the plate and mixed with 500 µl of liquified soft top agar (Nutrient Broth, NB, (Oxoid) with 7 g L^{-1} agar), precooled to 45 ºC in a water bath. Plates were gently stirred (20 rpm) to ensure an even distribution of bacterial cells in the inoculated wells. After the agar had solidified, plates were left for 10 min. under laminar flow to reduce moisture on the surface of the medium. Two µl of 10-times diluted phage tail-like particles (approximately 10^{10} particles mL^{-1}) purified from mitomycin-induced cultures of *D. dadantii* 3937 were spotted on the surface of the inoculated soft-top agar in the wells of the multitier plate.

Inoculated plates were incubated for 24 h at 28 ºC., then inspected the presence of a growth inhibition halo. The presence of the halo was interpreted as the susceptibility of the given strain to the phage tail-like particles (positive reaction). Two µl of sterile PBS was spotted on susceptible strain lawn as a negative control, resulting in no growth inhibition and no halo formation (negative reaction). The susceptibility of each bacterial strain was tested in triplicates, and the entire experiment was repeated two times with the same setup.

Determination of the bacterial killing rate

The velocity of bacterial killing by the phage tail-like particles was measured in 96-well plates (Nest) using the Epoch 2 microplate reader (BioTek). Twenty-five µl of a suspension containing phage tail-like particles (approximately 10^{11} particles mL^{-1}) in PBS pH 7.2 were added to 100 µl of 5 McF (approximately 10^{8} CFU mL^{-1}) bacterial suspension in PBS. Cells for the suspension originated from the overnight culture of a tested strain in TSB, harvested by centrifugation (5 min, 8000 RCF). The OD_{600} of the PBS suspensions was measured each minute for 2 hours. The plate was kept at 28 ºC throughout the experiment and shaken between measurements. Susceptible strain *Musicola paradisiaca* strain NCPPB 2511 was used as a positive control, and sterile PBS pH 7.2 without tailocins was used as a negative control. To obtain regression curves indicating the bacterial killing rate, the log-transformed values of OD_{600} from each time point were normalized to the log-transformed starting OD_{600}. The regression coefficient ($\Delta Log_{10}(OD_{600})min^{-1}$) was calculated for each of the obtained curves. For presentation, the killing rate was given at two representative time points (20 and 120 min) as the average % of the initial OD_{600} of the selected bacterial culture undergoing tailocin-caused killing (n=10).

Analysis of the phage tail-like particles with SDS-PAGE and ESI LC-MS/MS

Proteins constituting phage tail-like particles were separated using a 4-20% sodium dodecyl sulfate-polyacrylamide gradient gel (Mini-PROTEAN TGX Stain-Free Precast, Bio-Rad Hercules, USA) electrophoresis (SDS-PAGE) according to (*35*). For amino acid sequencing, protein bands were excised from the gel using a sterile scalpel, and excised agar pieces were placed in separate 1.5 mL Eppendorf tubes. In-gel digestion was performed according to standard protocol consisting of gel discoloration and removal of Coomassie staining, reduction/alkylation with dithiothreitol (DTT), and iodoacetamide (IAA), respectively (*36*). First, digestion was carried out overnight with trypsin (Promega Mass Spectrometry Grade Gold) at 37 °C. Then, the obtained tryptic peptides were eluted from the gel spots into the solution with sequential washing of gel pieces with 50 mM ammonium bicarbonate buffer, 5% formic acid in 50% acetonitrile, and 100% acetonitrile (*37*). Next, all samples were concentrated (SpeedVac), and the final cleanup was carried out using the StageTips method on the C18 phase to a 50% acetonitrile solution with 1% acetic acid (*38*). After concentrating the samples to 30 ml using the SpeedVac, fragmentation mass spectra were recorded for analysis. ESI LC-MS/MS analysis was performed on Triple Tof 5600+ mass spectrometer with DuoSpray Ion Source (AB SCIEX, Framingham, MA) connected to the Eksigent microLC (Ekspert MicroLC 200 Plus System, Eksigent, Redwood City, CA) equipped with the ChromXP C18CL column (3 µm, 120 Å, 150 × 0.5 mm). The microLC−MS/MS system was controlled by the AB SCIEX Analyst TF 1.6 software. Chromatographic separation was carried out for 30 min in a gradient program: (1) 0−1 min – 20% solvent B, (2) 1−26 min – 20−60% solvent B, (3) 26−28 min − 98% solvent B, (4) 29-30 min − 20% solvent B, where solvent A was 0.1% formic acid in water and solvent B 0.1% formic acid in acetonitrile. The identification of proteins present in the examined gel bands was carried out based on the obtained fragmentation spectra using the ProteinPilot software (v 4.5) or Peaks Studio and the appropriate protein database (UniProt *Dickeya dadanti 15.02.2023, unreviewed*) with an automated false discovery rate (1% FDR).

Bioinformatic analyses

Prediction of prophage regions in the genome of *D. dadantii* 3937 (Genbank accession: NC_014500.1) was conducted using PHASTER (42). The tailocin cluster and individual proteins it encodes were analyzed against NCBI databases using BLASTn and BLASTp (43). The topology of the tailocin cluster in *D. dadantii* 3937 was investigated using BioCyc (44). Phylogenomic analysis of the Soft Rot *Pectobacteriaceae* (SRP) genomes was based on core genome sequences and was performed using EDGAR ver. 3.0 (45) accessed via (https://edgar3.computational.bio.uni-giessen.de).

Stability of phage tail-like particles (*39-41*)

Phage tail-like particles were incubated for 24 hours in a set of temperatures (-80, -20, 4, 22, 28, 37, 42, 50, 65, and 80 °C), pH values (2, 5, 3.5, 7, 9, 10.5 and 12), and NaCl concentrations (0.01, 0.1, 1 and 5 M), following which their bacterial growth inhibitory activity was assessed by a spot test using susceptible *Musicola paradisiaca* strain NCPPB 2511 as described above. All tested samples had a total volume of 200 µl, and the initial concentration of phage tail-like particles was equal to 1/10 of the PEG-purified samples (approximately 10^{10} particles mL^{-1}). To obtain the test samples, phage tail-like particles were diluted by mixing a volume of 20 µL of PEG-purified samples with 180 µl of either PBS (temperature stability), PBS with pH modified by either HCl or NaOH to the desired values (pH stability), or water with NaCl (different concentrations of NaCl). The experiments were replicated three times, each with three technical repetitions per tested condition.

Effect of enzyme/detergent/organic solvent treatment on the activity of phage tail-like particles (*39, 41, 42*)

Phage tail-like particles were incubated for 1 hour at 37 °C (optimal temperature for the enzyme) with the following enzymes: proteinase K (Sigma-Aldrich, final concentration: 0.5

mg mL^{-1}), DNase (Sigma-Aldrich, final concentration: 10 U mL^{-1}), or lysozyme (Sigma-Aldrich, final concentration: 0.5 mg mL^{-1}), and at room temperature (22 °C) with a detergent - sodium dodecyl sulfate (SDS, Sigma Aldrich, final concentration: 1%), or an organic solvent – chloroform (POCH, 50% v/v). Subsequently, the remaining activity of treated phage tail-like particles was assessed in a spot test as described above. The processed samples had a total volume of 200 µL, with the initial concentration of phage tail-like particles equaling 1/10 of the PEG-purified sample (approximately 10^{10} particles mL^{-1}). The samples were prepared by mixing 20 µl of PEG-purified samples (about 10^{11} particles mL^{-1}) with the appropriate volume of the factor stock and making up to 200 µL with PBS. The exception were the chloroform-treated samples. In the latter case, 200 µL of sample containing phage tail-like particles were mixed on a shaker with 200 µL of chloroform during the whole incubation time. Prior to the spot test, the chloroform sample was centrifuged (5 min at 4000 RCF), and the aqueous phase was taken to enumerate the active phage-tail-like particles. The experiments were replicated three times, each with three technical repetitions per tested condition.

Binding of phage tail-like particles to nonviable bacterial cells (*41*)

Overnight bacterial cultures of susceptible (*M. paradisiaca* strain NCPPB 2511) and resistant (*D. dadantii* strain 3937) strains grown in TSB were washed twice with PBS buffer. Next, bacterial cells were killed by incubation with 5 mg mL^{-1} chloramphenicol (Sigma-Aldrich) for 60 min, with shaking (120 rpm, 28 ºC). The killing of the cells after 1 h was confirmed by plating 4 times 10 µL aliquots of treated bacterial culture on TSA plates and the incubation of inoculated plates at 28 ºC for 24 h to check the bacterial growth. After killing, the nonviable bacterial cells were again washed three times with PBS to remove the remaining antibiotic from the medium. Then the PEG-purified samples were diluted in the suspension of viable and nonviable susceptible and nonsusceptible bacteria to a final concentration of 1/10 of the initial concentration (approximately 10^{10} particles mL^{-1}) and incubated for 40 min, 120 rpm, 28 ºC. After the incubation, samples were filtered using a 0.2 µm PES (polyether sulfone)

membrane filter, following which the remaining bactericidal activity of tailocins was assessed by a spot test using susceptible *M. paradisiaca* strain NCPPB 2511. The experiments were replicated three times, each with three technical repetitions per tested condition.

Testing the influence of different pHs on the bactericidal activity of phage tail-like particles

The PEG-purified phage tail-like particles (approximately 10^{11} particles mL^{-1}) were diluted 10 times in PBS buffered to pH 2, 7, and 12 and incubated for 24 h at room temperature. After this time, the pH of each sample was adjusted to neutral pH (pH 7) using an equal volume of the buffered PBS. Such prepared solutions were incubated for 4 hours at room temperature and further tested for growth inhibitory activity using a spot test in three replicas as described above.

***Caenorhabditis elegans* toxicity assay**

To test whether phage tail-like particles produced by *D. dadantii* strain 3937 may influence the fitness of nematodes, the *Caenorhabditis elegans* liquid-killing assay was employed (*43*) with slight modifications. Briefly, the wild-type Bristol N2 strain of *C. elegans* nematode was obtained from the *Caenorhabditis* Genetic Center (CGC, University of Minnesota, Minneapolis, USA). The strain N2 was maintained as described before (*44, 45*) on Nematode Growth Medium (NGM) plates with *Escherichia coli* strain OP50 as a food source. The toxicity of the phage tail-like particles was tested on nematode cultures synchronized as described earlier (*46*). Briefly, nematode eggs were harvested from cultures treated with a mixture of 5M NaOH and 5.25% NaOCl (1:3, v:v) – a treatment that eliminates adult worms. Recovered eggs were hatched in an S-complete medium, and the nematodes were grown up to the L4 stage using *E. coli* OP50 as a food source. Next, the synchronized cultures were transferred into wells of a 96-well plate. The worms were counted under the microscope

(Leica MZ10f stereomicroscope, Leica) and placed ca. 30 worms per well. Each well was supplemented with PEG-purified and ultracentrifugation (1 h, 26 000 RCF, 4 ºC) purified phage tail-like particles prepared in an S-complete medium of concentration 10^{12} particles mL^{-1}. Nematode cultures grown without phage tail-like particles were used as control. The plates were incubated for 24 h in the dark at 25 °C. The average survival of nematodes in phage tail-like particles-supplemented cultures was compared to the control. The experiment was repeated two times with the same setup, and the results were averaged for analysis.

Statistical analysis

All statistical tests were conducted using either Past 4.13 software (*47*) or Microsoft Office Excel (www.office.com). The Shapiro-Wilk (*48*) and F-test (*49*) were used to test the normality and variance equality of data, respectively. For pairwise testing, the t-test (*50*) was applied for data with normal distribution and equal variances, the Welch test (*51*) was used for the normal distribution and unequal variances, and, finally, the U Mann-Whitney test (*52*) was applied for data that were not normally distributed. The one-way analysis of variance (ANOVA) (*53*) was used to compare more than two data groups. Levene's test (*54*) was used to test the homogeneity of variance, and the normality of the residuals was conducted using the Shapiro-Wilk test. Welch's one-way analysis of variance, followed by the Games-Howell post hoc test (*55*), was used for the data groups with non-homogeneous variance and normally distributed residuals. For groups with a non-homogeneous variance and without normally distributed residuals Kruscal-Wallis's one-way analysis of variance (*56*) followed by Dunn's post hoc test (*57*) was applied.

Results

D. dadantii 3937 produces phage tail-like particles

Cells of *D. dadantii* 3937 treated with mitomycin C were found to produce syringe-like macromolecular structures resembling bacteriophage tails. Following the convention, the tailocins produced by *D. dadantii* strain 3937 were named dickeyocins. Microscopic imaging using TEM and AFM revealed that these structures consist of a central rod-shaped core (tube) wrapped in a contractable sheath (Fig. 1). Both the tube and the sheath were built of multiple protein subunits, with a clearly visible helical arrangement of the subunits in the sheath. The average length of the dickeyocins produced by strain 3937 was 166±7 nm. When the sheath entirely covered the tube (in the extended, 'loaded' form), the individual dickeyocin has a diameter of 23±2 nm. When the sheath contracts, it revealed an internal tube of a length of 92±7 nm with an attached spike at the proximal end. Fibers were visible at the distal end of the sheath (Fig. 1).

The yield of phage tail-like particles purified from mitomycin-induced cells of *D. dadantii* 3937 equaled approx. 10^{11} particles mL^{-1} of culture. The particles could also be isolated from non-treated cells, indicating a basal production level. However, induction with mitomycin C increased the yield approx. 10-100 fold. We employed three different methods to estimate the concentration of phage-tail-like particles in the tested preparations. The results were consistent for all these applied methods, as well as for the independently-obtained batches of purified dickeyocins (Table S2). The average concentration from three independently obtained samples was 10^6 relative units (AU) mL^{-1}, 10^{11} killing particles $mL^{-1,}$ and 10^{11} particles mL^{-1}, according to the spot test, the Poisson distribution killing method, and the NanoSight measurements, respectively. Furthermore, comparing the results from the activity-based Poisson method and the direct particle count indicated that most phage-like particles purified from the cultures of *D. dadantii* strain 3937 were undamaged and in the extended ('loaded') form. This was in line with the microscopic observations done with TEM and AFM.

Phage tail-like particles from D. dadantii strain 3937 are phylogenetically related to the tail of P2 bacteriophage

Phage tail-like particles produced by *D. dadantii* 3937 were separated by SDS-PAGE. Eight cleary distinguishable bands were excised from the gel, and the digested peptides were analyzed by MS. This approach allowed us to identify bands contained peptides that could be directly mapped to six *D. dadantii* 3937 proteins with annotations implying their phage relationship: phage baseplate assembly protein (encoded in locus Dda3937_00029), baseplate assembly protein J (Dda3937_00030), tail fiber protein (Dda3937_04606), putative side tail fiber protein (Dda3937_03808), major sheath protein (Dda3937_03810), and major tail tube protein (Dda3937_03811) (Fig. 2). Genes encoding these six proteins were mapped to a single ca. 22-kb region in the genome of *D. dadantii* strain 3937 (GenBank accession number: NC_014500.1: range in the genome: 2,734,508 to 2,757,061). This genomic region contained 28 genes, from which 16 genes encoded various bacteriophage structural proteins.

The nucleotide sequence of the indicated 22-kb fragment in D. dadantii strain 3937 showed the highest similarity to a prophage region in *D. dadantii* strain XJ12 (100% query coverage (qc), 99.35% identity). Highly similar regions were also found in the genomes of several other strains of *D. dadantii*, as well as *D. solani*, *D. dianthicola*, and *D. fangzhongdai* (Data S1). Strains of *D. zeae* showed lower similarity levels, with query coverage between 54-76% and identity of 83-84%. A significant drop in score was observed for the next best hit – *Musicola paradisiaca* (formerly *Dickeya paradisiaca*). Other non-*Dickeya* microorganisms with regions showing some degree of homology included *Serratia* sp. ATCC 39006 (Data S1).

Importantly, at the nucleotide level, the tailocin region of strain 3937 showed no significant similarity to the known carotovorocin Er cluster of *P. carotovorum* Er (Genbank accession: AB045036) (*58*). Moreover, the amino acid sequence of the sheath protein of tailocin from strain 3937 showed only a 34% identity to that of carotovorocin Er, with a query coverage of 83%.

The ca. 22-kb cluster encoding tailocin from *D. dadantii* strain 3937 was also surveyed against the nucleotide collection narrowed down to viral sequences (NCBI taxid: 10239), yielding low similarity scores (7% query coverage, 78% identity for the best hit).

Furthermore, in an attempt to find undomesticated phages related to the studied tailocin, we have searched the viral database at a protein level, using three structural proteins of tailocin as queries: sheath protein (WP_013318223), tail tube protein (WP_013318224), and baseplate assembly protein J (WP_013318212). Based on this search, proteins building the phage tail-like particle from *D. dadantii* 3937 showed homology to proteins of *Salmonella* phages SW9 and PSP3, *Erwinia* phage Etg, *Enterobacteria* phage fiAA91-ss, *Peduovirus* (bacteriophage) P2, several *Escherichia* and *Yersinia* phages, as well as to multiple poorly-characterized phages of class *Caudoviricetes*, derived from the human metagenome (Data S1). The best-characterized phage with high homology to tailocin from strain 3937 was the *Enterobacteria* phage P2 – a *Myoviridae* phage that infects *Escherichia coli* and other hosts, including *Salmonella* and *Klebsiella* (*59, 60*). For the three investigated tailocin proteins, their amino acid identity towards their P2 homologs ranged from 70-79%, with 100% query coverage (Data S2). Therefore, we used the *Enterobacteria* P2 bacteriophage as a reference to assign the function to proteins in phage tail-like particles isolated from *D. dadantii* strain 3937, as well as to investigate genetic rearrangements in the tailocin cluster in comparison to a fully-functional phage P2 (Fig. 2C). Tailocin cluster in the genome of strain 3937 lacked sequences associated with the phage head (proteins O, M, N, L), as well as the tape measure protein. There was also a difference in the genetic content of the intergenic region of the tail, as well as low homology of proteins building the tail fibers (31% query coverage, 54% identity).

Following the present naming convention, we named the newly characterized phage tail-like particles from *D. dadantii* 3937 **dickeyocins P2D1** (P2-like Dickeyocin 1).

Dickeyocins P2D1 express bactericidal activity exclusively against members of Soft Rot Pectobacteriaceae

Forty-one SRP strains were tested for sensitivity to dickeyocins P2D1 (Table S1). Bactericidal activity was observed against eight strains (*D. dadantii* subsp. *dieffenbachie* strain NCPPB 2976, *D. dianthicola* strains NCPPB 3534 and IPO 980, *D. undicola* CFBP 8650, *D. zeae* strains NCPPB 3532 and 3531, *D. oryzae* strain CSL RW192, and *Musicola paradisiaca* strain NCPPB 2511 (old name: *Dickeya paradisiaca* strain NCPPB 2511), but not against any of the *Pectobacterium* spp. tested (Table S1, Fig. 3). Likewise, phage tail-like particles P2D1 were inactive against any of the non-SRP strains included in the screening assay: 7 *Enterobacteriaceae* strains (*Serratia marcescens* ATCC 14756, *Citrobacter freundii* ATCC 8090, *Escherichia coli* ATCC 8739, *Escherichia coli* ATCC 25922, *Escherichia coli* OP50, *Klebsiella quasipneumoniae* ATCC 700603, *Klebsiella aerogenes* ATCC 51697), 3 *Pseudomonas* spp.: (*Pseudomonas aeruginosa* PA14, *Pseudomonas aeruginosa* PAO1, *Pseudomonas donghuensis* P482), and *S. aureus* ATCC 25923 indicating their limited range of bactericidal activity (Fig. 3).

P2D1 rate of killing is bacterial species-dependent

We determined the killing kinetics of eight susceptible strains treated with P2D1. The share of intact cells at two time points: 20 and 120 minutes post treatment in shown in Fig. S1. In all the cases, the killing of the susceptible cells was fast. In the first 20 minutes, the fastest cell killing caused by the presence of P2D1 was observed for *D. dianthicola* strain IPO 980 (ca. 60% reduction of cell numbers as measured by the OD_{600} changes). In contrast, the slowest killing caused by dickeyocins was observed for *D. dianthicola* strain NCPP 3534 (ca. 22% reduction of cell numbers). For the other 6 strains tested, on average, a 45 to 60% reduction in cell numbers was observed at the same time (20 min.). After 120 min-incubation of bacterial cells with dickeyocins, a decrease in cell numbers in a range of 50 to 60% was observed for all strains tested (Fig. S1).

P2D1 dickeyocins directly puncture the cell envelope of susceptible bacterial strains

We assessed the direct interaction of P2D1 and susceptible bacterial cells of *M. paradisiaca* strain NCPPB 2511 at the single-cell level using transmission electron microscopy (TEM). In the reproducible microscopic assays, it was cleanly visible that P2D1 dickeyocins can adsorb to bacterial cell envelope (Fig. 4 AB), which is followed by puncturing the outer cell membrane (resulting from the conformational change of P2D1 from extended 'loaded' to contracted form) (Fig. 4 CD), creating a pore connecting the cytoplasm of the cell with the external environment and leading eventually to the death of the attacked cell.

Dickeyocins P2D1 are able to bind to nonviable (dead) bacterial cells

The dead cell adsorption assay was employed to investigate whether the P2D1 dickeyocins can adsorb to nonviable (dead) and viable bacterial cells of the susceptible or resistant bacterial species. P2D1 dickeyocins were incubated either with viable or chloramphenicol-killed cells of *M. paradisiaca* strain NCPPB 2511 (susceptible strain) or with viable or antibiotic-killed cells of *D. dadantii* strain 3937 (resistant strain) for 40 min. After that, the activity of the remaining P2D1 dickeyocins (in AU) in the medium was measured. Incubation of P2D1 dickeyocins both with the dead and viable cells of *M. paradisiaca* strain NCPPB 2511 resulted in the total loss of the P2D1 activity, indicating that they can bind equally efficiently to viable as well as nonviable (dead) cells of the susceptible bacterium. No adsorption of P2D1 dickeyocins to dead and alive cells of the resistant *D. dadantii* 3937 was observed during the experiment (Fig. S2).

Production of dickeyocins P2D1 is not associated with T6SS

To check whether the P2D1 dickeyocins production in *D. dadantii* strain 3937 depends on the type VI secretion system (T6SS), tailocins were induced from the *D. dadantii* strain 3937 mutant A5587 (*61*) that carries an insertional mutation in the *tssK* gene (type VI secretion

system baseplate subunit TssK) – an essential subunit of the type VI secretion apparatus (*62*). The tailocins obtained from the *D. dadantii* mutant A5587 using the same induction method were morphologically indistinguishable and comparatively active compared to P2D1 dickeyocins induced from these produced by the wild-type *D. dadantii* strain 3937 (Fig. S3). These results suggest that at least mutation in the *tssK* gene, essential for the proper function of T6SS, does not affect the P2D1 production, morphology, and functionality.

Activity of P2D1 dickeyocins is modulated by environmental conditions and enzyme treatments

Dickeyocins P2D1 were stable at temperatures between 4 and 42 °C, showing no significant activity loss following 24 h incubation. Increasing the temperature to 50 °C led to a 32-fold activity loss, with a complete lack of activity observed following 24 h incubation at 65 and 80 °C (Fig. 5 A). Likewise, a single freeze-thaw cycle negatively affected the stability of P2D1. Freezing at -20 °C resulted in a 128-fold drop in activity, with no bactericidal effect following freezing at -80 °C (Fig. 5 A). We tested the stability of P2D1 under 7 different pH conditions (2, 3.5, 5, 7, 9, 10.5, and 12). The particles remained active after 24 h incubation in pHs ranging from 3.5 to 12. However, their bactericidal properties were lost at pH 2 (Fig. 5 B). Osmotic pressure generated by NaCl in concentrations between 0.01 to 5 M during a 24 h incubation had no adverse effect on the activity of P2D1 when compared to control (dickeyocins in PBS containing 0.137 M NaCl and 0.0027 mM KCl). Contrary, incubation of P2D1 particles in deionized water led to a 4-fold loss in activity (Fig. 5 C). P2D1 phage tail-like particles were significantly ($p<0.05$) affected by the 1-hour treatment with proteinase K and chloroform (4-fold and 2-fold loss of activity, respectively) and ultimately lost their activity after incubation in 1% SDS. Contrarily, both lysozyme and DNase treatments did not influence dickeyocin activity (Fig. 5 D).

Dickeyocins P2D1 are not reusable after their inactivation with a low pH

To check whether the inactivated by a low pH P2D1 dickeyocins are resuscitated to their active (extended, 'loaded') form, we diluted the pH 2-treated, inactive P2D1 in PBS buffered to pH 12 in a ratio that resulted in the environment of neutral pH. Such a pH change did not reconstitute the activity of P2D1 dickeyocins.

Dickeyocins P2D1 are nontoxic for Caenorhabditis elegans

At the end point of the killing assay, the average survival rate of *C. elegans* cultivated in the presence of P2D1 dickeyocins was ca. 98-99% and was not significantly statistically different from the survival rate recorded for the nematodes grown without dickeyocins (control). The survival rate was not P2D1 concentration-dependent, as similar survival rates were recorded for all dickeyocin concentrations tested (Fig. S4). Furthermore, the P2D1 dickeyocins did not show bactericidal activity against *E. coli* OP50 – a nematode food source.

Discussion

Our understanding of the mechanisms underlying bacterial competitive behaviors remains limited. Although numerous bacterial species are known to produce and exploit phage tail-like particles (tailocins) for their competitive advantage, little is known of how commonly such entities are used by plant-pathogenic bacteria, including pectinolytic, necrotrophic SRP pathogens, to boost their environmental fitness (*9, 10*). This study explored the presence and activity of phage tail-like particles in one of the broadest characterized member of the Soft Rot *Pectobacteriaceae* family – strain *D. dadantii* 3937. We identified and characterized in detail a novel phage tail-like particle – dickeyocin P2D1, produced by this strain upon mitomycin C treatment. Although phage tail-like particles were initially superficially characterized in a limited number of *Dickeya* spp. (=strains of *Erwinia chrysanthemi*, but not strain 3937) isolated from several crop and ornamental plants in the past (1960s and 1970s) (*63*), these particles were not characterized in detail, probably due to

the absence of essential molecular techniques at that time. To our knowledge, this is the first report providing detailed information about tailocins produced by *D. dadantii* strain 3937.

Transmission electron microscopy and atomic force microscopy applied to P2D1 dickeyocin revealed structures resembling the tails of *Myoviridae* bacteriophages (*64*). Detailed microscopic observations revealed that P2D1 consists of a rigid and contractible sheath, a core with apical spike protein, and fibers attached at one end of the particle. In the following experiments, P2D1 could adsorb to both alive and nonviable (dead) cells of susceptible bacteria but was unable to adsorb to resistant cells. We also showed that P2D1 dickeyocins remain active under a wide range of conditions. They were stable under different temperatures, pHs, and salt concentrations, as well as when incubated in the presence of lysozyme and DNase. P2D1 were, however, inactivated by SDS, chloroform, and treatment with proteinase K. Interestingly, the very low pH caused an irreversible inactivation of P2D1. Furthermore, the T6SS *D. dadantii* mutant (*61*), when screened for tailocin synthesis, was not affected in P2D1 production, indicating that P2D1 and T6SS are not functionally interconnected in this strain (*9*). P2D1 dickeyocins, therefore, have a typical morphology and expresses features similar to those of other R-type phage tail-like particles described so far for a large group of bacteria, including *Escherichia coli* (*65*), *Burkholderia cenocepacia* (*28*), *Pseudomonas aeruginosa (10)*, *Proteus vulgaris* (*66*) and *Yersinia enterocolitica (67)*. Likewise, phage-tail-like bacteriocins were also identified in the case of *Pectobacterium* spp. (*58, 68, 69*) - bacteria closely related to *Dickeya* spp. The one bast characterized to date is carotovorocin Er isolated from *P. carotovorum* (*70, 71*). Interestingly, as shown in this study, despite the morphological similarities of the P2D1 and carotovorocin Er and the rather close phylogenetic relationship and the lifestyle shared by the producer strains, both tailocins show little sequence homology to one another. It suggests that P2D1 and carotovorocin Er originated from different phage-related ancestors and that the ability to produce tailocins was acquired several times and independently by various members of the SRP family.

The cluster encoding P2D1 dickeyocin in *D. dadantii* strain 3937 expresses high homology with the cluster encoding the tail of *Enterobacteria* phage P2 which indicates that these two probably had a common ancestor. Phage P2 is a temperate bacteriophage belonging to the *Myoviridae* family, commonly found in genomes of strains belonging to the *Proteobacteria* phylum (*60*). Its presence has been reported at least in 127 genera in 32 *Proteobacteria* families (*72*), indicating its extreme ubiquitousness in the bacterial world. Accordingly, R-type tailocins resembling the tail of the P2 phage were extensively studied and are now the best characterized to date (*5, 10*). To explore the occurrence of R-type tailocins in SRP, we searched available *Dickeya* spp. and *Pectobacterium* spp. genomes for regions carrying phage tail-like genes homologous to those identified in P2D1 and exhibiting organizational similarity. Our analysis revealed the presence of P2D1-like clusters in several *Dickeya* spp. strains, including *D. solani*, *D. dianthicola, D. zeae*, and *D. fangzhongdai*. The P2D1-like clusters were, however, absent in all *Pectobacterium* spp. genomes as well as in genomes of the other bacterial species unrelated to SRP analyzed in our study. The lack of the P2D1 cluster both in *Pectobacterium* spp. and in bacteria phylogenetically distant to SRP may indicate a strong and sustained phylogenetic association between P2D1 and *Dickeya* spp. This is perhaps unexpected given that various *Dickeya* and *Pectobacterium* are often present in the same environment (e.g., soil, water, plant surface) (*19*). Under such conditions, horizontal gene transfer would frequently occur between phylogenetically close strains of different SRP species (*73*).

The restricted presence of cluster encoding dickeyocin P2D1 in genomes of *Dickeya* spp. aligns with its narrow bactericidal activity. In our study, P2D1 targeted exclusively strains representing five *Dickeya* species and *Musicola paradisiaca* (former *Dickeya paradisiaca*) but not any other bacteria tested. It is worth mentioning that the P2D1-susceptible SRP strains were killed at different time-depending efficiency and that this efficiency was unrelated to phylogenetical distance between strains. This is in line with other studies (*40, 74, 75*). For example, as evidenced in the case of pyocins, that are tailocins

produced by *Pseudomonas* spp., their range activity is usually restricted to kin strains (*9*). Similar observations were made concerning phage tail-like particles isolated from *Escherichia coli* (*76*) and *Yersinia enterocolitica (67)*. Contrarily, emerging reports characterized tailocins targeting different species of the same genus and/or the ones with even an interspecies bactericidal range. Such phage tail-like particles were characterized in *Burkholderia cenocepacia* active against other *Burkholderia* species (*28*) and *P. fluorescens* that produces tailocins active against *Xanthomonas vesicatoria* (*77*). The quite narrowed target range of P2D1 may be a bit of a surprise, considering that multiple species of SRP bacteria are often founded in the same infected plant in direct proximity (*78-80*). Under such conditions, various species of SRP are expected to experience extensive competition (*81*). They should therefore be equipped with means to combat kin strains *in situ*. It can be speculated that in multiple infections, *Dickeya* spp. and *Pectobacterium* spp. compete using mechanisms unrelated to phage-tail-like particles, as reported previously (*82, 83*), but this subject requires more experimental data to draw firm conclusions.

Our study revealed that P2D1 dickeyocins are produced without induction with mitomycin C, but the induction boosts the tailocin production ten to one hundred times. To precisely estimate the concentration of P2D1 particles, we used a well-established Poisson distribution killing method (*33, 34*) and a new approach developed in this study. The Poisson distribution killing method is an indirect counting method as it relies on the number of survivors in tailocin-treated bacterial suspensions. The important upside of using indirect methods to assess the quality of tailocin preparations is that they provide the number of active ('loaded') tailocin particles in a sample. In this study, we have complemented the indirect counting approach by direct enumeration of tailocin particles with NanoSight NS300. Performing a direct particle count does not require culturing time, and using killing-based methods enables the estimation of the fraction of active tailocins in preparation. To our knowledge, NanoSight has never been used before to evaluate the quality and the active fraction of tailocin preparations.

One of the immediate applications of P2D1 dickeyocins to consider would be controlling SRP infections in crops (*84*). The biggest practical problem of applying tailocins, including the ones described in this study, to control plant pathogens, is their narrow bactericidal range. This can be, at least partially, overcome by using cocktails of tailocins with different bactericidal ranges, similarly as it is done with bacteriophages (*85*). Nevertheless, even with this limitation, tailocins have already been recognized as potential antibacterial agents in various applications (*86, 87*). They have several benefits compared to other biological control agents known to date (*84*). One of the biggest advantages of such particles is their incapacity to proliferate on-site after application. Likewise, tailocins cannot unintentionally spread genes via transduction or recombination mechanisms because they do not contain DNA or RNA. It must also be pointed out that the extreme selectivity of the tailocins mentioned above may be their gain as it assures that applying phage tail-like particles will not negatively affect other and often beneficial bacteria present in the same niche. Likewise, as evidenced in our study in which P2D1 tailocins were nontoxic to a model eukaryotic organism – *C. elegans*, they are probably safe also to other eukaryotic organisms present in soil and/or on plants (*88*).

Additional studies are needed to fully explore the potential of P2D1 dickeyocins in practice, targeting production, the long-term effectiveness, and consistency of control under field conditions, including stability, formulation, and eco-toxicological risks. Finally, elucidation of the P2D1 synthesis regulation would be of value to better understand the role of phage tail-like particles in the ecology and fitness of SRP bacteria under natural and agricultural conditions.

Competing Interest Statement

The authors declare no competing interests.

Acknowledgments

This research was financially supported by the National Science Center, Poland (Narodowe Centrum Nauki, Polska) via a research grant SONATA BIS 10 (2020/38/E/NZ9/00007) to Robert Czajkowski. The authors would like to express their gratitude to Dr. Nicole Hugouvieux-Cottee-Pattat (Laboratory of Microbiology Adaptation and Pathogenesis (UMR 5240) CNRS, Université Lyon 1 & INSA de Lyon, France) for providing strain A5587 (*D. dadantii* strain 3937 *tssK*::*uidA* kanR) for this study and Prof. Alfonso Jaramillo and Dr. Cristina Ramos (De Novo Synthetic Biology Lab, Institute for Integrative Systems Biology (I2SysBio-CSIC)) for providing valuable information on the P2 phage.

Figures

Fig. 1 The morphology of phage tail-like particles from *D. dadantii* 3937. Images were obtained using TEM (A-C) and AFM (D-F). The individual panels show: (**A**) particles in an extended (active) form. Arrows indicate the positioning of fibers; (**B**) contracted particles indicated by arrows; (**C**) phage tail-like particles disintegrated by heat treatment (50 □C); Arrows indicate: **a** – empty sheath with a hollow inner channel, **b** – tube (core) separated from the sheath; (**D**) two extended particles. A fragment of the photo was magnified to display the helical arrangement of protein subunits in the sheath; (**E**) a contracted molecule in an AFM image; (**F**) an extended particle with an arrow pointing at the tube-attached spike.

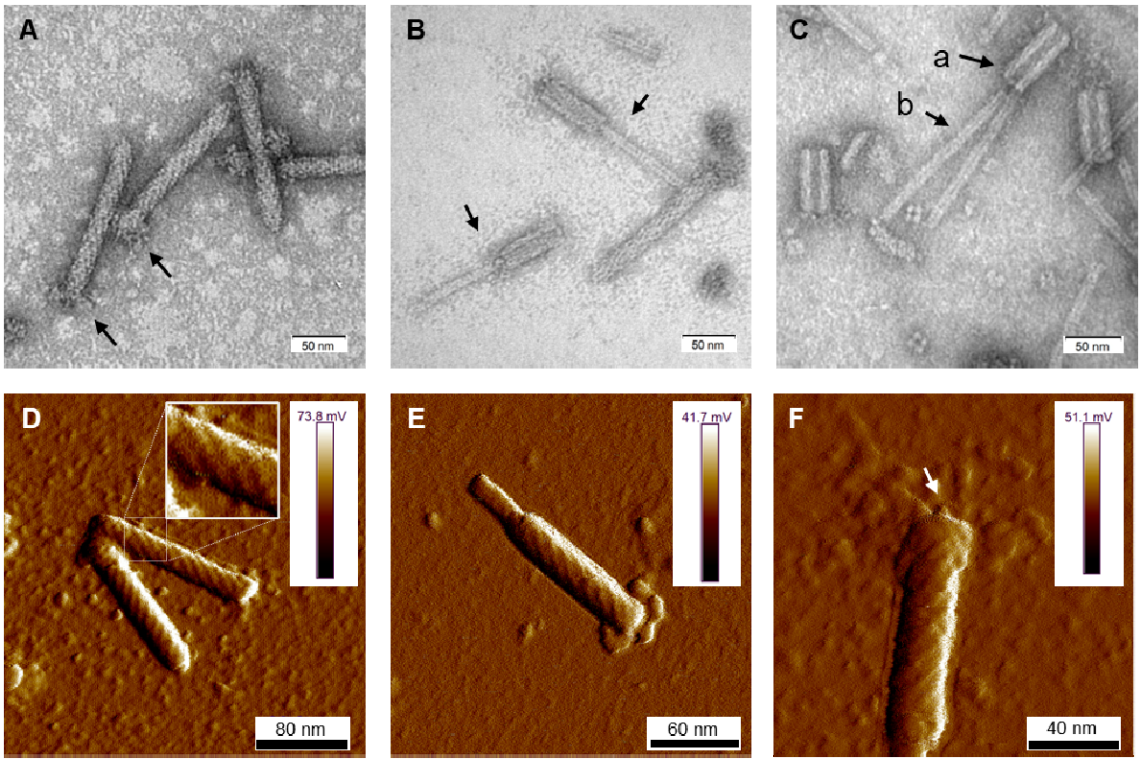

Fig. 2 The building blocks of phage tail-like particles of *D. dadantii* strain 3937 and their encoding genes in relation to those of the *Enterobacteria* P2 bacteriophage.

Panel A shows a schematic representation of the structure of the P2 phage, together with the nomenclature of the building proteins. The graph was prepared based on Cristi and Calendar, 2016 (PMID: 27144088, https://pubmed.ncbi.nlm.nih.gov/27144088/). WJIDX – baseplate proteins, F_I – sheet, H - fiber, F_{II} – tube, V – spike, T – tape measure protein, Q – portal protein, N – major capsid protein, O – capsid scaffold, L – head completion protein.

Panel B shows: **I.** an SDS-PAGE separation of proteins from mitomycin-induced cultures of *D. dadantii* 3937. Bands containing proteins homologous to those of the P2 phage are provided with the respective protein designations; **II.** schematic representation of extended and contracted forms of dickeyocin P2D1; **III.** TEM micrographs of extended and contracted forms of dickeyocin P2D1.

Panel C shows the alignment between the complete genome sequence of the P2 phage (NC_001895; 33 593 bp) and a region of the same length in the genome of *D. dadantii* 3937 (NC_014500.1; range: 2723487 to 2757061). The numbering of genes in *D. dadantii* corresponds to the numbering of loci in the genome (locus tag prefix DDA3937_RS). Homologous proteins are marked with the same color.

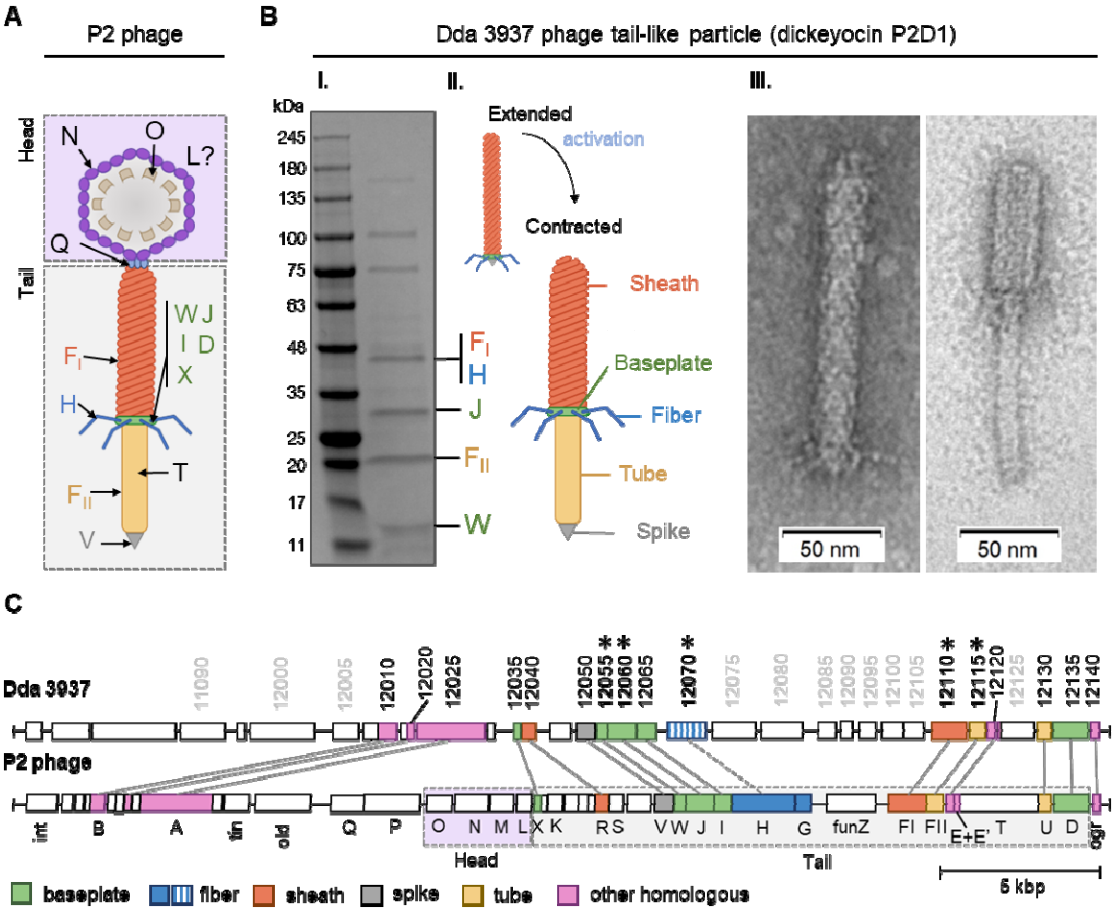

Fig. 3 Target range of phage tail-like particles from *D. dadantii* 3937. Strains susceptible to P2D1 dickeyocin were marked with a plus (+). A phylogenetic tree for 41 SRP strains was obtained using EDGAR 3.2. It was built out of a core of 1616 genes per genome (nucleotide sequences), 66256 genes in total. The core had 1560951 bp per genome, 63998991 in total. The lengths of the branches do not reflect the phylogenetic distance. All analyzed *Pectobacterium* spp. were collapsed. This included 16 strains: *P. cacticida* CFBP 3628, *P. fontis* CFBP 8629, *P. betavasculorum* CFBP 2122, *P. peruviense* CFBP 5834, *P. atrosepticum* SCRI1043, *P. atrosepticum* NCPPB 549, *P. parmentieri* CFBP 8475, *P. parmentieri* SCC3193, *P. polonicum* DPMP 315, *P. punjabense* CFBP 8604, *P. actinidiae* LMG 26003, *P. brasiliense* LMG21371, *P. polaris* NCPPB 4611, *P. versatile* CFBP 6051, *P. carotovorum* CFBP 2046, *P. aroidearum* NCPPB 929.

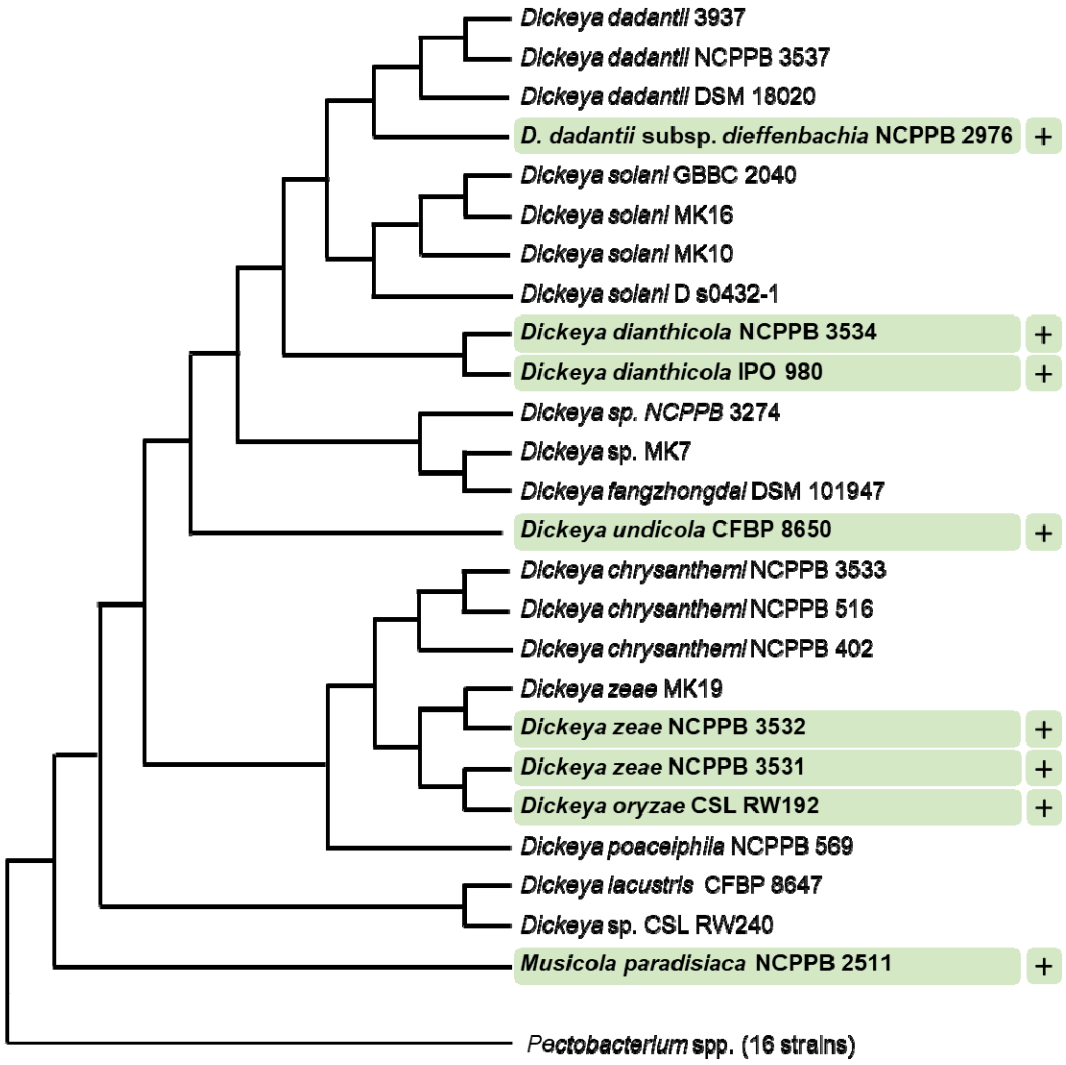

Fig. 4 Interaction of P2D1 dickeyocins with the cells of a susceptible strain *M. paradisiaca* NCPPB strain 2511, evaluated using transmission electron microscopy (TEM). Bacterial cells of *M. paradisiaca* NCPPB 2511 from overnight culture in TSB were harvested and washed with PBS. Such prepared cells were incubated with PEG-purified dickeyocins (approximate concentration in bacterial suspension 10^6 particles mL^{-1}) for 20 min, followed by obtaining images with TEM. For all panels, the TEM images on the right are the enlarged sections of the original micrographs on the left. Arrows indicate P2D1 attached to the surface of bacterial cells, either in extended (A-B) or contracted (C-D) form.

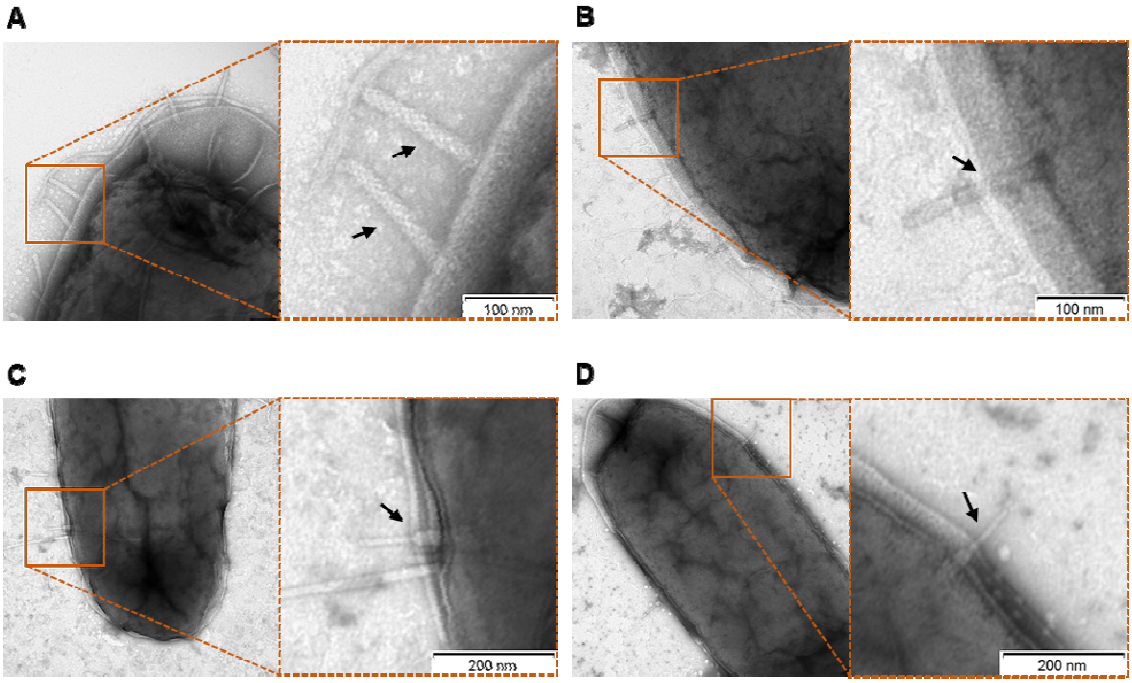

Fig. 5 Stability of P2D1 dickeyocins from *Dickeya dadantii* strain 3937 upon different treatments. The graphs show the influence of temperature (A), pH (B), salinity (C), as well as enzymatic digestion (proteinase K, DNase, and lysozyme), chloroform treatment, and SDS detergent (D) on bactericidal activity of P2D1 against *M. paradisiaca* NCPPB 2511. For temperature, pH/osmolarity, and enzyme/detergent/organic solvent treatments, dickeyocins stored in PBS pH 7, were used as a control. The results are shown as a box plot; whiskers reflect the maximum and minimum, box sides reflect the first and third quartile and the bars reflect medians. Points indicate particular measurements (n=9). The asterisks (*) represent statistically significant differences ($p<0.05$) between the treatment and the control using the Mann-Whitney test.

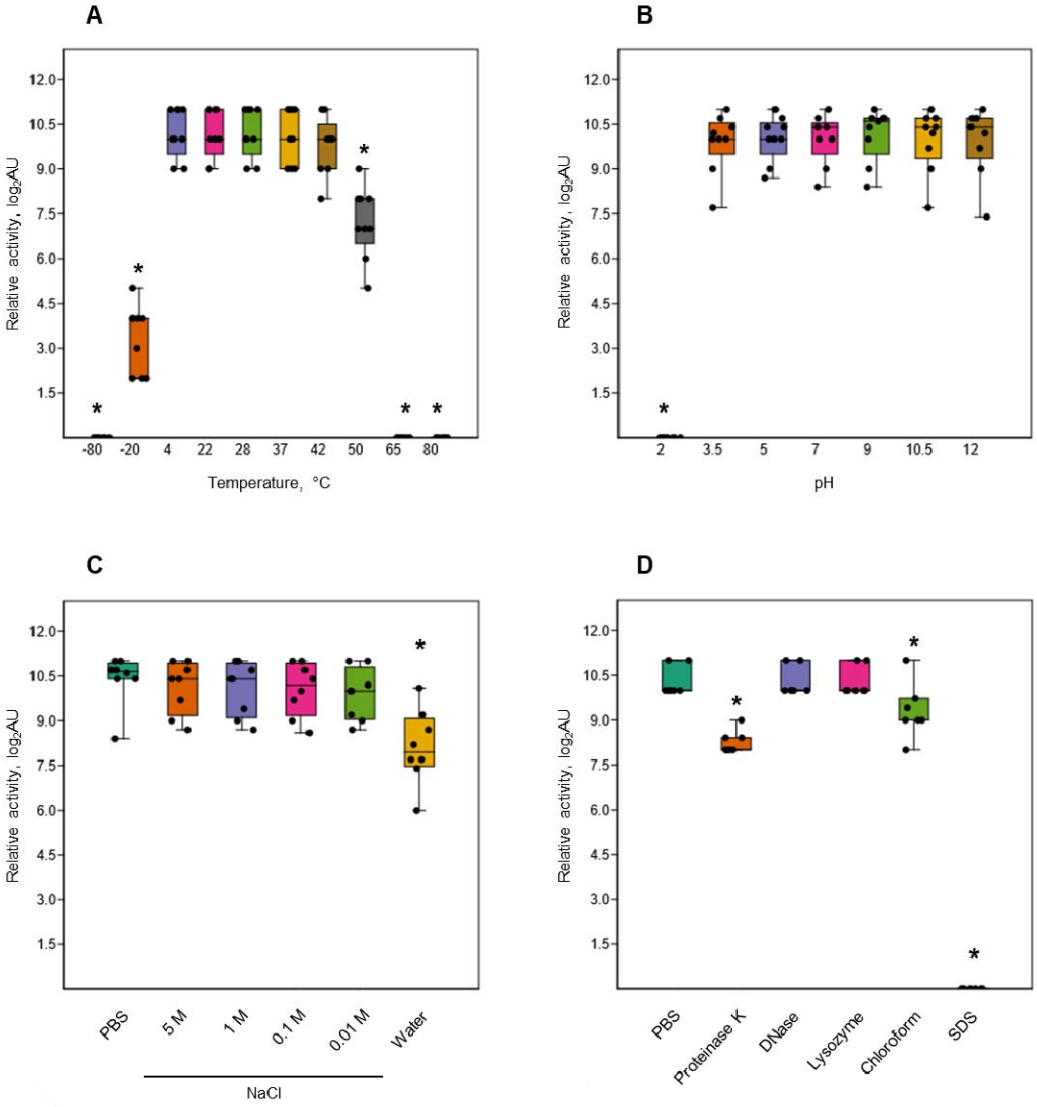

References

1. F. A. Gorter, M. Manhart, M. Ackermann, Understanding the evolution of interspecies interactions in microbial communities. *Philos Trans R Soc Lond B Biol Sci* **375**, 20190256 (2020).
2. A. E. Little, C. J. Robinson, S. B. Peterson, K. F. Raffa, J. Handelsman, Rules of engagement: interspecies interactions that regulate microbial communities. *Annu Rev Microbiol* **62**, 375-401 (2008).
3. A. Wagner, Competition for nutrients increases invasion resistance during assembly of microbial communities. *Mol Ecol* **31**, 4188-4203 (2022).
4. M. A. Bauer, K. Kainz, D. Carmona-Gutierrez, F. Madeo, Microbial wars: Competition in ecological niches and within the microbiome. *Microb Cell* **5**, 215-219 (2018).
5. E. T. Granato, T. A. Meiller-Legrand, K. R. Foster, The Evolution and Ecology of Bacterial Warfare. *Curr Biol* **29**, R521-R537 (2019).
6. M. Ghoul, S. Mitri, The Ecology and Evolution of Microbial Competition. *Trends Microbiol* **24**, 833-845 (2016).
7. M. E. Hibbing, C. Fuqua, M. R. Parsek, S. B. Peterson, Bacterial competition: surviving and thriving in the microbial jungle. *Nat Rev Microbiol* **8**, 15-25 (2010).
8. R. M. Stubbendieck, P. D. Straight, Multifaceted Interfaces of Bacterial Competition. *J Bacteriol* **198**, 2145-2155 (2016).
9. S. Patz *et al.*, Phage tail-like particles are versatile bacterial nanomachines - A mini-review. *J Adv Res* **19**, 75-84 (2019).
10. D. Scholl, Phage Tail-Like Bacteriocins. *Annu Rev Virol* **4**, 453-467 (2017).
11. P. Ge *et al.*, Atomic structures of a bactericidal contractile nanotube in its pre- and postcontraction states. *Nat Struct Mol Biol* **22**, 377-382 (2015).
12. M. G. K. Ghequire, R. De Mot, The Tailocin Tale: Peeling off Phage Tails. *Trends Microbiol* **23**, 587-590 (2015).
13. M. G. K. Ghequire, R. De Mot, Ribosomally encoded antibacterial proteins and peptides from Pseudomonas. *FEMS Microbiology Reviews* **38**, 523-568 (2014).
14. N. Morales-Soto, S. Gaudriault, J.-C. Ogier, K. R. V. Thappeta, S. Forst, Comparative analysis of P2-type remnant prophage loci in Xenorhabdus bovienii and Xenorhabdus nematophila required for xenorhabdicin production. *FEMS Microbiology Letters* **333**, 69-76 (2012).
15. J. Liu, P. Chen, C. Zheng, Y. P. Huang, Characterization of maltocin P28, a novel phage tail-like bacteriocin from Stenotrophomonas maltophilia. *Appl Environ Microbiol* **79**, 5593-5600 (2013).
16. G. W. Yao *et al.*, A Broad-Host-Range Tailocin from Burkholderia cenocepacia. *Appl Environ Microbiol* **83**, e03414-03416 (2017).
17. D. Gebhart *et al.*, A modified R-type bacteriocin specifically targeting Clostridium difficile prevents colonization of mice without affecting gut microbiota diversity. *mBio* **6**, 10.1128/mbio.02368-02314 (2015).
18. Y. Michel-Briand, C. Baysse, The pyocins of Pseudomonas aeruginosa. *Biochimie* **84**, 499-510 (2002).
19. F. Van Gijsegem, J. M. van der Wolf, I. K. Toth, *Plant Diseases Caused by Dickeya and Pectobacterium Species*. (Springer, 2021).
20. A. O. Charkowski, The Soft Rot *Erwinia*. *Plant-Associated Bacteria* **part 3**, 423-505 (2007).

21. A. O. Charkowski, The Changing Face of Bacterial Soft-Rot Diseases. *Annu Rev Phytopathol* **56**, 269-288 (2018).
22. M. C. M. Perombelon, Potato diseases caused by soft rot erwinias: an overview of pathogenesis. *Plant Pathology* **51**, 1-12 (2002).
23. A. Kotoujansky, M. Lemattre, P. Boistard, Utilization of a thermosensitive episome bearing transposon TN10 to isolate Hfr donor strains of Erwinia carotovora subsp. chrysanthemi. *J Bacteriol* **150**, 122-131 (1982).
24. R. Samson *et al.*, Transfer of Pectobacterium chrysanthemi (Burkholder et al. 1953) Brenner et al. 1973 and Brenneria paradisiaca to the genus Dickeya gen. nov. as Dickeya chrysanthemi comb. nov. and Dickeya paradisiaca comb. nov. and delineation of four novel species, Dickeya dadantii sp. nov., Dickeya dianthicola sp. nov., Dickeya dieffenbachiae sp. nov. and Dickeya zeae sp. nov. *Int. J. Syst. Evol. Microbiol.* **55**, 1415-1427 (2005).
25. A. Kotoujansky, Molecular genetics of pathogenesis by soft-rot Erwinias. *Annu. Rev. Phytopathol.* **25**, 405-430 (1987).
26. S. Reverchon, G. Muskhelisvili, W. Nasser, in *Progress in Molecular Biology and Translational Science*, M. San Francisco, B. San Francisco, Eds. (Academic Press, 2016), vol. 142, pp. 51-92.
27. S. Reverchon, W. Nasser, Dickeya ecology, environment sensing and regulation of virulence programme. *Environ Microbiol Rep* **5**, 622-636 (2013).
28. G. W. Yao *et al.*, A Broad-Host-Range Tailocin from Burkholderia cenocepacia. *Appl Environ Microbiol* **83**, (2017).
29. K. L. Hockett, D. A. Baltrus, Use of the Soft-agar Overlay Technique to Screen for Bacterially Produced Inhibitory Compounds. *J Vis Exp*, e55064 (2017).
30. J. Vacheron, C. M. Heiman, C. Keel, Live cell dynamics of production, explosive release and killing activity of phage tail-like weapons for Pseudomonas kin exclusion. *Commun Biol* **4**, 87 (2021).
31. P. Bartnik *et al.*, Resistance of Dickeya solani strain IPO 2222 to lytic bacteriophage PhiD5 results in fitness tradeoffs for the bacterium during infection. *Sci Rep* **12**, 10725 (2022).
32. D. Sokolova *et al.*, Spontaneous mutations in hlyD and tuf genes result in resistance of Dickeya solani IPO 2222 to phage varphiD5 but cause decreased bacterial fitness and virulence in planta. *Sci Rep* **13**, 7534 (2023).
33. S. R. Williams, D. Gebhart, D. W. Martin, D. Scholl, Retargeting R-Type Pyocins To Generate Novel Bactericidal Protein Complexes. *Applied and Environmental Microbiology* **74**, 3868-3876 (2008).
34. M. Kageyama, K. Ikeda, F. Egami, Studies of a Pyocin. Iii. Biological Properties of the Pyocin. *J Biochem* **55**, 59-64 (1964).
35. J. Sambrook, E. F. Fritsch, T. Maniatis, *Molecular cloning: a laboratory manual*. (1989).
36. A. Golebiowski *et al.*, Functionalization of Alpha-Lactalbumin by Zinc Ions. *ACS Omega* **7**, 38459-38474 (2022).
37. A. R. Goldman *et al.*, Proteome Analysis Using Gel-LC-MS/MS. *Curr Protoc Protein Sci* **96**, e93 (2019).
38. R. Schmidt, A. Sinz, Improved single-step enrichment methods of cross-linked products for protein structure analysis and protein interaction mapping. *Anal Bioanal Chem* **409**, 2393-2400 (2017).
39. J. Smarda, O. Benada, Phage tail-like (high-molecular-weight) bacteriocins of Budvicia aquatica and Pragia fontium (Enterobacteriaceae). *Appl Environ Microbiol* **71**, 8970-8973 (2005).

40. A. Príncipe, M. Fernandez, M. Torasso, A. Godino, S. Fischer, Effectiveness of tailocins produced by Pseudomonas fluorescens SF4c in controlling the bacterial-spot disease in tomatoes caused by Xanthomonas vesicatoria. *Microbiological Research* **212-213**, 94-102 (2018).
41. C. F. Gonzalez, B. S. Kunka, Plasmid-Associated Bacteriocin Production and Sucrose Fermentation in Pediococcus acidilactici. *Appl Environ Microbiol* **53**, 2534-2538 (1987).
42. S. Fischer *et al.*, Characterization of a phage-like pyocin from the plant growth-promoting rhizobacterium Pseudomonas fluorescens SF4c. *Microbiology (Reading)* **158**, 1493-1503 (2012).
43. N. V. Kirienko, B. O. Cezairliyan, F. M. Ausubel, J. R. Powell, in *Pseudomonas Methods and Protocols*, A. Filloux, J.-L. Ramos, Eds. (Springer New York, New York, NY, 2014), pp. 653-669.
44. T. Stiernagle, *Maintenance of C. elegans*. WormBook (2006), vol. http://www.wormbook.org/, pp. 1-11
45. D. M. Krzyzanowska *et al.*, Compatible Mixture of Bacterial Antagonists Developed to Protect Potato Tubers from Soft Rot Caused by Pectobacterium spp. and Dickeya spp. *Plant Dis* **103**, 1374-1382 (2019).
46. M. Porta-de-la-Riva, L. Fontrodona, A. Villanueva, J. Ceron, Basic Caenorhabditis elegans methods: synchronization and observation. *J Vis Exp*, e4019 (2012).
47. Ø. Hammer, D. A. T. Harper, P. D. Ryan, PAST: paleontological statistics software package for education and data analysis. *Palaeontologia electronica* **4**, 9 (2001).
48. S. S. Shapiro, M. B. Wilk, An Analysis of Variance Test for Normality (Complete Samples). *Biometrika* **52**, 591-& (1965).
49. Q. Shen, J. Faraway, An F test for linear models with functional responses. *Statistica Sinica* **14**, 1239-1257 (2004).
50. D. Semenick, Tests and measurements: The T-test. *Strength & Conditioning Journal* **12**, 36-37 (1990).
51. B. L. Welch, The generalisation of student's problems when several different population variances are involved. *Biometrika* **34**, 28-35 (1947).
52. H. B. Mann, D. R. Whitney, On a test of whether one of two random variables is stochastically larger than the other. *The annals of mathematical statistics*, 50-60 (1947).
53. A. Ross, V. L. Willson, in *Basic and advanced statistical tests*. (Brill, 2017), pp. 21-24.
54. B. B. Schultz, Levene's test for relative variation. *Systematic Zoology* **34**, 449-456 (1985).
55. P. Mégevand. (2022).
56. P. E. McKight, J. Najab, Kruskal‐wallis test. *The corsini encyclopedia of psychology*, 1-1 (2010).
57. G. D. Ruxton, G. Beauchamp, Time for some a priori thinking about post hoc testing. *Behavioral ecology* **19**, 690-693 (2008).
58. K. Yamada *et al.*, Nucleotide sequences and organization of the genes for carotovoricin (Ctv) from Erwinia carotovora indicate that Ctv evolved from the same ancestor as Salmonella typhi prophage. *Biosci Biotechnol Biochem* **70**, 2236-2247 (2006).
59. G. Bertani, Studies on lysogenesis. I. The mode of phage liberation by lysogenic Escherichia coli. *J Bacteriol* **62**, 293-300 (1951).
60. G. E. Christie, R. Calendar, Bacteriophage P2. *Bacteriophage* **6**, e1145782 (2016).

61. M. Golanowska, CNRS, Université Lyon 1 & INSA de Lyon, France, University of Gdansk, Gdansk, Poland, INSA, Lyon, France (2015).
62. V. S. Nguyen *et al.*, Type VI secretion TssK baseplate protein exhibits structural similarity with phage receptor-binding proteins and evolved to bind the membrane complex. *Nature Microbiology* **2**, 17103 (2017).
63. E. Echandi, Production, Properties, and Morphology of Bacteriocins fromErwinia chrysanthemi. *Phytopathology* **69**, 1204-1207 (1979).
64. M. Sanz-Gaitero, M. Seoane-Blanco, M. J. van Raaij, Structure and function of bacteriophages. *Bacteriophages: Biology, Technology, Therapy*, 19-91 (2021).
65. H. Mennigmann, Electronmicroscopy of the anti-bacterial agent produced by Escherichia coli 15. *MICROBIOLOGY* **41**, 151-154 (1965).
66. H. L. Coetzee, H. C. De Klerk, J. N. Coetzee, J. A. Smit, Bacteriophage-tail-like particles associated with intra-species killing of Proteus vulgaris. *J Gen Virol* **2**, 29-36 (1968).
67. E. Strauch *et al.*, Characterization of enterocoliticin, a phage tail-like bacteriocin, and its effect on pathogenic Yersinia enterocolitica strains. *Appl Environ Microbiol* **67**, 5634-5642 (2001).
68. J. K. Choi, I. O. Kim, Properties of carotovoricin H, a bacteriocin from Erwinia carotovora subsp. carotovora. *The Plant Pathology Journal* **4**, 33-39 (1988).
69. S. Kamimiya, K. Izaki, H. Takahashi, Bacteriocins in Erwinia aroideae with tail like structure of bacteriophages. *Agricultural and Biological Chemistry* **41**, 911-912 (1977).
70. S. Kamimiya, K. Izaki, H. Takahashi, Bacteriocins inErwinia aroideaewith Tail Like Structure of Bacteriophages. *Agricultural and Biological Chemistry* **41**, 911-912 (2014).
71. H. A. Nguyen, J. Kaneko, Y. Kamio, Temperature-dependent production of carotovoricin Er and pectin lyase in phytopathogenic Erwinia carotovora subsp. carotovora Er. *Biosci Biotechnol Biochem* **66**, 444-447 (2002).
72. S. R. Casjens, J. H. Grose, Contributions of P2- and P22-like prophages to understanding the enormous diversity and abundance of tailed bacteriophages. *Virology* **496**, 255-276 (2016).
73. I. K. Toth *et al.*, in *Plant Diseases Caused by Dickeya and Pectobacterium Species*, F. Van Gijsegem, J. M. van der Wolf, I. K. Toth, Eds. (Springer International Publishing, Cham, 2021), chap. Chapter 2, pp. 13-37.
74. P. C. Fagundes *et al.*, The antimicrobial peptide aureocin A53 as an alternative agent for biopreservation of dairy products. *Journal of Applied Microbiology* **121**, 435-444 (2016).
75. L. Chopra, G. Singh, K. Kumar Jena, D. K. Sahoo, Sonorensin: A new bacteriocin with potential of an anti-biofilm agent and a food biopreservative. *Scientific Reports* **5**, 13412 (2015).
76. E. Tantoso *et al.*, To kill or to be killed: pangenome analysis of Escherichia coli strains reveals a tailocin specific for pandemic ST131. *Bmc Biology* **20**, 1-26 (2022).
77. A. Principe, M. Fernandez, M. Torasso, A. Godino, S. Fischer, Effectiveness of tailocins produced by Pseudomonas fluorescens SF4c in controlling the bacterial-spot disease in tomatoes caused by Xanthomonas vesicatoria. *Microbiol Res* **212-213**, 94-102 (2018).
78. T. Ge, F. Ekbataniamiri, S. B. Johnson, R. P. Larkin, J. Hao, Interaction between Dickeya dianthicola and Pectobacterium parmentieri in Potato Infection under Field Conditions. *Microorganisms* **9**, 316 (2021).

79. M. C. M. Perombelon, in *Bacterial disease of Potato: report of the planning conference on Bacterial diseases of potato*. (CIP, Lima, Peru, 1988).
80. M. C. M. Pérombelon, Potato blackleg: Epidemiology, host-pathogen interaction and control. *Tijdschrift Over Plantenziekten* **98**, 135-146 (1992).
81. D. Y. Shyntum *et al.*, The Impact of Type VI Secretion System, Bacteriocins and Antibiotics on Bacterial Competition of Pectobacterium carotovorum subsp. brasiliense and the Regulation of Carbapenem Biosynthesis by Iron and the Ferric-Uptake Regulator. *Front Microbiol* **10**, 2379 (2019).
82. R. Czajkowski *et al.*, Virulence of 'Dickeya solani' andDickeya dianthicolabiovar-1 and -7 strains on potato (Solanum tuberosum). *Plant Pathology* **62**, 597-610 (2013).
83. B. Ma *et al.*, Host range and molecular phylogenies of the soft rot enterobacterial genera pectobacterium and dickeya. *Phytopathology* **97**, 1150-1163 (2007).
84. Y. Becker *et al.*, Bacteria producing contractile phage tail-like particles (CPTPs) are promising alternatives to conventional pesticides. *Journal für Kulturpflanzen* **74**, 85-93 (2022).
85. S. T. Abedon, K. M. Danis-Wlodarczyk, D. J. Wozniak, Phage Cocktail Development for Bacteriophage Therapy: Toward Improving Spectrum of Activity Breadth and Depth. *Pharmaceuticals (Basel)* **14**, (2021).
86. D. Scholl, D. W. Martin, Jr., Antibacterial efficacy of R-type pyocins towards Pseudomonas aeruginosa in a murine peritonitis model. *Antimicrob Agents Chemother* **52**, 1647-1652 (2008).
87. H. M. Behrens, A. Six, D. Walker, C. Kleanthous, The therapeutic potential of bacteriocins as protein antibiotics. *Emerg Top Life Sci* **1**, 65-74 (2017).
88. E. M. Balciunas *et al.*, Novel biotechnological applications of bacteriocins: a review. *Food control* **32**, 134-142 (2013).